

Article

Selective Recovery of Molybdenum over Rhenium from Molybdenite Flue Dust Leaching Solution Using PC88A Extractant

Ali Entezari-Zarandi ^{1,2,*}, Dariush Azizi ^{1,3}, Pavel Anatolyevich Nikolaychuk ⁴ , Faiçal Larachi ¹ and Louis-César Pasquier ³ 

¹ Department of Chemical Engineering, Université Laval, Québec, QC G1V 0A6, Canada; Dariush.Azizi@ete.inrs.ca (D.A.); faical.larachi@gch.ulaval.ca (F.L.)

² Centre Technologique des Résidus Industriels (CTRI), Rouyn-Noranda, QC J9X 0E1, Canada

³ Center Eau Terre Environnement, Institut National de la recherche scientifique (INRS), Québec, QC G1K 9A9, Canada; louis-cesar.pasquier@inrs.ca

⁴ Lehrstuhl für Thermodynamik und Energietechnik, Universität Paderborn, Warburger Straße 100, 33098 Paderborn, Germany; npa@csu.ru

* Correspondence: Ali.Entezarizarandi@cegepat.qc.ca; Tel.: +1-819-762-0931 (ext. 1737)

Received: 31 August 2020; Accepted: 23 October 2020; Published: 26 October 2020



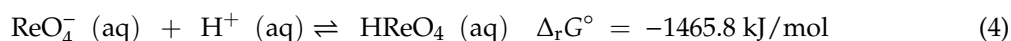
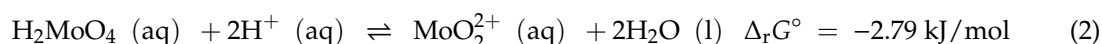
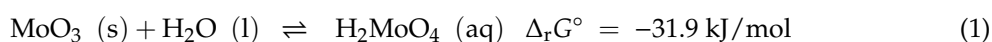
Abstract: Selective solvent extraction of molybdenum over rhenium from molybdenite (MoS₂) flue dust leaching solution was studied. In the present work, thermodynamic calculations of the chemical equilibria in aqueous solution were first performed, and the potential–pH diagram for the Mo–Re–SO₄²⁻–H₂O system was constructed. With the gained insight on the system, 2-ethylhexyl phosphonic acid mono-(2-ethylhexyl)-ester (PC88A) diluted in kerosene was used as the extractant agent. Keeping constant the reaction temperature and aqueous-to-organic phase ratio (1:1), organic phase concentration and pH were the studied experimental variables. It was observed that by increasing the acidity of the solution and extractant concentration, selectivity towards Mo extraction increased, while the opposite was true for Re extraction. Selective Mo removal (+95%) from leach solution containing ca. 9 g/L Mo and 0.5 g/L Re was achieved when using an organic phase of 5% PC88A at pH = 0. No rhenium was coextracted during 10 min of extraction time at room temperature. Density functional theory (DFT) calculations were performed in order to study the interactions of organic extractants with Mo and Re ions, permitting a direct comparison of calculation results with the experimental data to estimate selectivity factors in Mo–Re separation. For this aim, PC88A and D2EHPA (di-(2-ethylhexyl) phosphoric acid) were simulated. The interaction energies of D2EHPA were shown to be higher than those of PC88A, which could be due to its stronger capability for complex formation. Besides, it was found that the interaction energies of both extractants follow this trend considering Mo species: MoO₂²⁺ > MoO₄²⁻. It was also demonstrated through DFT calculations that the interaction energies of D2EHPA and PC88A with species are based on these trends, respectively: MoO₂²⁺ > MoO₄²⁻ > ReO₄⁻ and MoO₂²⁺ > ReO₄⁻ > MoO₄²⁻, in qualitative agreement with the experimental findings.

Keywords: rhenium; molybdenum; solvent extraction; separation; hydrometallurgy

1. Introduction

Molybdenum (Mo) is a strategic metal that has an extensive demand in different branches of the industry. Rhenium (Re) is also a strategic metal, although less common with wide applications in the oil industry (e.g., production of reforming catalyst) and in heat-resistant alloys (e.g., aerospace). Typically, in Mo sulphide concentrates (molybdenite, MoS₂), Re coexisting with varying concentrations

ranging from 0.001% to 0.1% is identified [1]. Upon roasting, molybdenite transforms into technical-grade Mo oxide, while Re content escapes the reactor in the form of Re_2O_7 , which partly deposits in the filters alongside the flue dust. Scrubbing the flue gases and leaching flue dusts are effective methods to recover Re values. Such solutions typically have 5–10 g/L Mo and 0.4–0.9 g/L Re. Due to similar chemical properties, Mo–Re separation is a challenge, and a number of studies have been devoted to introducing ad hoc technologies in this regard. Ion exchange and solvent extraction are the most used separation methods [2]. However, the separation of Mo and Re from liquors obtained from leaching molybdenite roasting flue dust is an essential step in order to produce high-purity final products, such as ammonium perrhenate and ammonium (para) molybdate. The following hydrolysis and acidic reactions illustrate the reactants/products involved in the leaching of flue dust [3,4]:



At high acid concentration, the anionic oxyspecies of rhenium (i.e., perrhenate ion (ReO_4^-)) is highly stable, and other possible short-life species readily hydrolyse to it. On the other hand, molybdenum forms cationic oxyspecies (MoO_2^{2+}) at high acid concentration, evolving into neutral and anionic species with increasing pH [5].

Many attempts have been made on Mo and Re separation. Solvating extractant TBP (tributyl phosphate) is used for Re removal in near-zero pH, followed by Mo removal employing commercial extractant LIX984N [6]. Stepwise removal of Mo with TBP was conducted at pH near 2, and afterwards, Re was removed at pH lower than 0 [7]. Similarly, the coextraction of molybdenum and rhenium by N235 (tri-octyl amine) and their separation from stripping solution by using D201 ion-exchange resin (containing quaternary ammonium group [$\text{N}-(\text{CH}_3)_2\text{C}_2\text{H}_4\text{OH}$]) has been reported [8]. Selective extraction of rhenium over molybdenum from alkaline solutions has also been studied by employing an organic phase composed of 20% N235 and 30% TBP diluted in kerosene [9]. An organic phase composed of 5 vol% N235 (in kerosene) was found to selectively recover Re over Mo at equilibrium pH 0.0 [10]. Table 1 lists recent attempts to separate Re and Mo from their aqueous mother liquor.

The use of appropriate solvents is a challenging problem. The commercially available extractant Cyanex 923 has been shown to be an appropriate choice for the purpose of rhenium recovery [11]. The lower solubility of Cyanex 923 in water compared with that of TBP (0.05 to 0.4 g/L at 25 °C, respectively) and its complete miscibility with diluents at low temperature are mentioned as some of its advantages over other solvents such as TOPO (trioctylphosphine oxide) and Aliquat 336. Pathak et al. [12] studied the extraction behaviour of molybdenum from acidic radioactive wastes using PC88A. They found that by increasing HNO_3 concentration in the aqueous phase, Mo extraction decreases, while increasing the organic concentration until 0.15 M causes an increase in metal extraction.

In the present work, the application of PC88A (2(ethylhexyl)phosphonic acid mono-2(ethylhexyl)-ester) extractant was studied on Mo–Re separation in solutions obtained from leaching molybdenite flue dust under various conditions of organic concentration and aqueous solution acidity. Next, the performance of PC88A was compared with that of D2EHPA using both experimentation and density functional theory simulations.

Table 1. Literature on Mo and Re solvent extraction.

Extractant/Diluent	Acidity	Selectivity	Ref.
N235 + TBP/kerosene	pH = 9	Re over Mo 15 g/L Mo + 0.1 g/L Re 97.6%: 1.6%	[9]
N235/kerosene	pH = 0	Re over Mo	[10]
Cyanex 923/kerosene	pH = 0 HCl	Re	[11]
N235 + isooctanol/kerosene	pH = 0 HNO ₃	Re over Mo	[13]
LIX 63/kerosene	pH = 2–6 H ₂ SO ₄	Mo over W	[14]
D2EHPA/kerosene	pH = 3–4 H ₂ SO ₄	Mo over W	[15]
TBP/kerosene	pH = 2 pH = 0 H ₂ SO ₄	Mo over Re Re over Mo	[7]
TBP/kerosene	pH = 0 <3.0 M HCl	Re over Mo and V Re and Mo over V	[16]
TBP/kerosene	pH = 1.5 pH = –0.3 H ₂ SO ₄	Mo over Re Re over Mo	[1]
Alamine 304-1/Anysol-150	pH = 2–3 H ₂ SO ₄	Re over Mo 260–280 mg/L Re + 80–90 mg/L Mo	[17]
PC88A/ <i>n</i> -dodecane	0.1–4.0 M HNO ₃	Mo 0.01 mol/L	[12]
PC88A/Sulfonated kerosene	pH = –0.2 ~ 0.5 HCl	Mo	[18]

N235 = tri-octyl amine, TBP = tributyl phosphate, Cyanex 923 = trialkylphosphine oxide, LIX 63 = 5,8-diethyl-7-hydroxy-6-dodecanone oxime, D2EHPA = di-(2-ethylhexyl)phosphoric acid, Alamine 304-1 = tri-*n*-dodecyl amine, PC88A = 2(ethylhexyl)phosphonic acid mono-2(ethylhexyl)-ester.

2. Experimentation

2.1. Materials and Reagents

Babakan Ferromolybdenum Co. (Kerman, Iran) kindly provided molybdenite flue dust. Table 2 lists the main chemical composition of the flue dust sample. Deionised water (industrial grade) was used as the leaching agent. D2EHPA and PC88A extractants were analytical-grade products kindly provided by Farapoyan Isatis Co., Yazd, Iran. Kerosene (Tehran Refinery, Tehran, Iran) was used as diluent, and sulphuric acid and sodium hydroxide (Merck) were the pH-adjusting agents used in our protocols. An iron-rich copper solvent extraction raffinate sample (NICICO, Tehran, Iran) was also used to investigate the possibility of selective separation of Mo from present metal impurities.

Table 2. Composition of flue dust before leaching (ppm).

Component	As	Ca	Cu	Fe	Mg	Mo	Na	Pb	Re	S	Se	Zn
Content	785	3670	3450	1720	775	36.6%	2380	1260	3980	25.2%	6650	242

2.2. Flue Dust Leaching

Molybdenite flue dust leaching was carried out in a 5 L glass reactor equipped with a mechanical agitation system (600 rpm) and a water jacket. The pulp density and reaction temperature were 20 wt.% and 80 °C, respectively. A mixture of water and alcohols (e.g., ethyl or methyl alcohol) was found to help in the selective leaching of rhenium over molybdenum [19]. Selective leaching has the advantage of separation of desired values from the very first steps of hydrometallurgical treatment [20]. However, for the sake of simplicity in the current work, only deionised water of industrial quality was used to eliminate the probable effect of additives on the solvent extraction step. It is worth noting that the application of acidic medium for leaching is unfavourable due to excessive introduction of Mo and other impurities, such as Fe, into the solution [21]. The leach liquor samples (5 mL without compensation) were withdrawn at predetermined intervals and immediately filtered through a medium quantitative filter paper to be analysed for Re and Mo content after required dilution with deionised water. The pH was monitored over the filtered samples in order to understand its variations during the leaching process (Figure 1a). After 360 min of contact, the remaining hot solution was filtered under gentle vacuum and cooled down to room temperature in order to obtain the stock solution. The solution underwent a series of colour changes in the course of leaching (Appendix A, Figure A1). It first became pale yellow, then turned into green, and finally dark blue. Metal recovery and pH variation profiles are presented in Figure 1b. Stock solution composition is listed in Table 3.

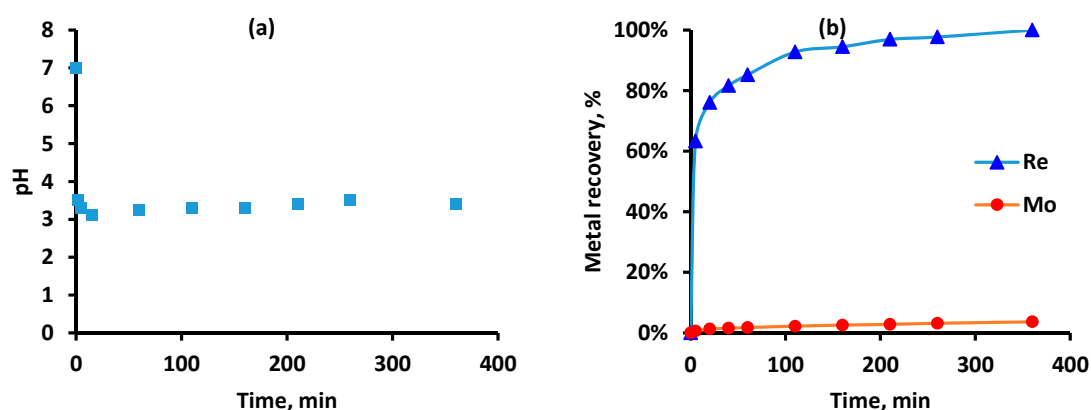


Figure 1. Dissolution of metal oxides from flue dust: (a) pH variations and (b) metal recovery over time. $T = 85\text{ }^{\circ}\text{C}$, $t = 360\text{ min}$, 600 rpm.

Table 3. Chemical composition of stock solution.

Element	Mo	Re	Cu	Se	Fe
Concentration (ppm)	9150	455	2.5	6.2	2000

2.3. Experimental Procedure

Different concentrations of PC88A diluted in kerosene (i.e., 5, 15, and 30 vol%) were used to test the influence of the extractant concentration on Re–Mo extraction and separation. Likewise, various pH classes of stock solution (i.e., −1, 1, 0, 3, 7, and 9) were prepared using sulphuric acid and sodium hydroxide. All the solvent extraction experiments were performed at room temperature. For all extraction experiments, an organic-to-aqueous ratio of 1:1 (25 mL for each) was imposed. Good contacting between phases was achieved during 10 min of mixing under magnetic stirring (600 rpm) with a cross-shaped magnet (3 cm in diameter) in 250 mL capacity beakers. Agitated mixtures were then transferred to a separation funnel and retained there for another 10 min before aqueous phase separation and chemical analysis. However, the phase separation time was

measured to be in the order of 20 to 30 s. It is worth noting that for the case of pH values of 7 and 9, the solution was filtered before the experiment to separate formed iron precipitates.

2.4. Chemical Analysis

An inductively coupled plasma optical emission spectrometer (ICP-OES) was used to determine the Re and Mo concentrations in all aqueous solutions. The Cu and Fe contents were measured by atomic absorption spectrometry (AAS) where necessary. The samples were treated prior to analysis by the addition of appropriate amounts of nitric acid, followed by dilutions to a predetermined volume.

2.5. Thermodynamic Analysis of Equilibria in Aqueous Solution

Thermodynamic calculations were performed in order to identify the equilibrium aqueous species in the leaching stock solutions. According to Table 3, the total contents of molybdenum and rhenium in the solution are equal to ~9 g/L (9.4×10^{-2} mol/L) and ~0.5 g/L (2.7×10^{-3} mol/L), respectively. The calculations were performed at pH values of 2, 1, 0, and -1, which correspond to the total content of sulphuric acid ranging from 6.5×10^{-3} to 10.09 mol/L. The concentrations of different dissociation products of sulphuric acid were calculated as presented in Appendix B and used to calculate the ionic strength of the solutions.

The activity coefficients of both ReO_4^- and MoO_2^{2+} ions were calculated from the extended Debye-Hückel theory [22]. The values of the effective radii of the ions and the values for water dielectric constant were taken from references [23,24], respectively. The calculation details are presented in Appendix B. As can be seen, the average activities of molybdenum species are ~0.01 mol/L, and those of rhenium species are ~0.001 mol/L. The activities of sulphur species have no effect on the chemical equilibria.

The chemical and electrochemical equilibria in the leaching stock solutions were presented in the form of convenient potential-pH diagrams. The diagrams for molybdenum [4] and sulphur [25] were constructed earlier. The thermodynamic characteristics of the reactions for rhenium were calculated using data from [26].

The potential-pH diagram for the Mo-Re-SO₄²⁻-H₂O system is plotted at 25 °C, air pressure of 1 bar and the activities of the molybdenum species 0.01 mol/L, the activities of the rhenium species 0.001 mol/L, and the activities of the sulphur species 0.1 mol/L, and presented in Figure 2.

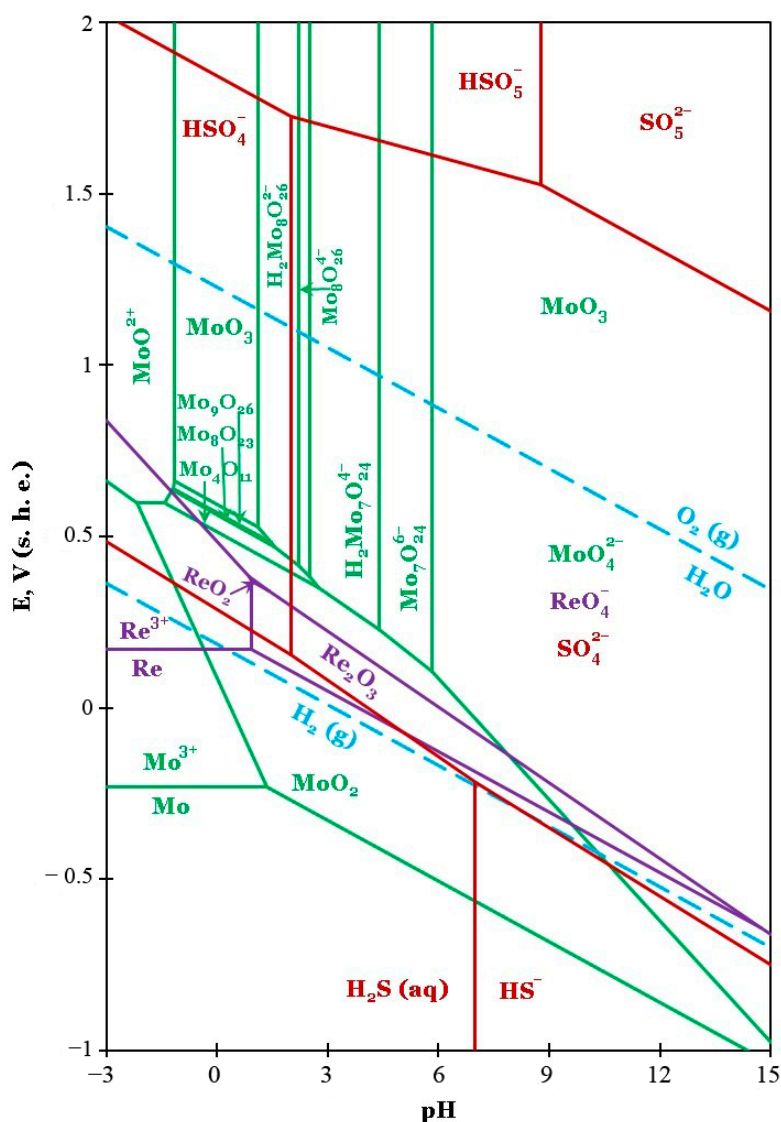


Figure 2. The potential–pH diagram for the Mo–Re–SO₄^{2−}–H₂O system is plotted at 25 °C, air pressure of 1 bar and the activities of molybdenum, rhenium, and sulphur species equal to 0.01, 0.001, and 0.1 mol/L, respectively.

2.6. DFT Computational Details

Density functional theory (DFT)-based simulations were conducted using Dmol3 module implemented in Material Studio 2016 software package. The structures of nonsolvated and water-solvated forms of MoO₄^{2−}, MoO₂²⁺, and ReO₄[−] were optimised in the aqueous pregnant solution. For the interactions in the organic phase, only the optimised structures of MoO₄^{2−}, MoO₂²⁺, and ReO₄[−], deprived of their inner-sphere water molecules, were considered [26]. Similarly, the structures of PC88A and D2EHPA were optimised in the organic phase. The complexation (or interaction) energies in the aqueous ($E_{C/w}$) and organic ($E_{C/o}$) phases of the complex species were determined as follows [27]:

$$E_{C/w} = E_{\text{Species} + \text{Reagent}/w} - E_{\text{Species}/w} - E_{\text{Reagent}/o} \quad (5)$$

$$E_{C/o} = E_{\text{Species} + \text{Reagent}/o} - E_{\text{Species}/o} - E_{\text{Reagent}/o} \quad (6)$$

where $E_{\text{Species} + \text{Reagent}/w}$ is the total energy after complex formation in the aqueous phase between water-solvated species aqua-complexes and two reagent (PC88A and D2EHPA) species; $E_{\text{Species} + \text{Reagent}/o}$

is the total energy after complex formation between species and two reagent (PC88A and D2EHPA) species in the organic phase; $E_{\text{Species/w}}$ is the energy of optimised solvated MoO_4^{2-} , MoO_2^{2+} , and ReO_4^- aqua-complexes; $E_{\text{Species/o}}$ is the energy of optimised MoO_4^{2-} , MoO_2^{2+} , and ReO_4^- species in the organic phase; and $E_{\text{reagent/o}}$ is the energy of solvated PC88A and D2EHPA optimised in the organic phase. Note the “w” and “o” index solvent parameterizations in Equations (5) and (6) for the conductor-like screening model (COSMO) used as an implicit solvation model to account for the aqueous, interfacial, and organic environments of the simulated structures. In this regard, dielectric constant was considered to be 78.54 (water) [24] and 1.8 (kerosene) for simulations in the aqueous phase and the organic phase, respectively.

The generalised gradient approximation (GGA) with Perdew-Burke-Ernzerhof exchange-correlation density functional (PBEsol) was used to describe the exchange correlation interactions. The double numerical plus polarization (DNP) basis was selected. The self-consistent field (SCF) convergence was fixed to 2×10^{-6} (0.005 kJ/mol), and the convergence criteria for the energy, maximum force, and maximum displacement were set to 2×10^{-5} Ha (0.05 kJ/mol), 0.05 Ha/Å, and 0.002 Å, respectively. No special treatment of core electrons was considered, and all the electrons were included in the calculations. In addition, a smearing value was fixed at 5×10^{-3} through calculation. In the spin-unrestricted condition, the calculation was performed by the use of various orbitals for different spins. Besides, the initial value for the number of unpaired electrons for each atom was taken from the formal spin introduced for each atom. In this situation, the starting value can be subsequently optimised throughout the calculations. Maximum SCF interactions and calculation interactions were set at 2000 and 1000, respectively, and calculation of the interactions step was set to 0.3 Å. It is worth mentioning that different initial positions were considered for all cases during DFT simulations, and only the most stable configuration and results have been reported. Besides, it is worthy to mention that similar studies in rhenium/ molybdenum solvent extraction have not been conducted based on the authors’ best of knowledge.

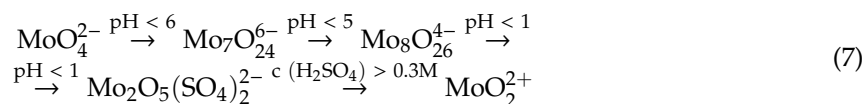
3. Results and Discussion

3.1. Effects of pH and Organic Phase Concentration

A potential–pH equilibrium diagram for the Mo–Re– SO_4^{2-} – H_2O system is presented in Figure 2. It can be inferred that soluble perrhenate (ReO_4^-) ion is the dominant species over the whole pH range. However, for the case of Mo, several cationic and anionic species may be present depending on the solution pH. In a neutral to alkaline region, MoO_4^{2-} is the predominant species, while moving towards the acidic region, complex anionic species will form.

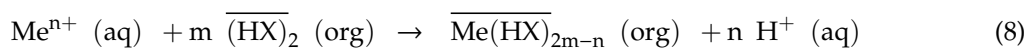
The precipitation of molybdenum oxide MoO_3 in the acidic media was not experimentally observed because of the formation of complex compounds of molybdenum (VI) with sulphate anions [28,29].

Variation of oxidation states of Mo over pH could simply be presented as follows [30]:



These complexes of molybdenum (VI) with sulphate were not included in the thermodynamic calculations due to lack of information on their stability constants.

PC88A, a close analog of D2EHPA, is an acidic organophosphorus extractant that is typically present as a dimer with a noticeable potential to extract cationic molybdenum species through ion exchange. The highly hydrophobic organic anion forms an organic neutral complex with the metal ions that are present in the aqueous phase:



where $(HX)_2$ represents the dimeric form of PC88A. Due to the formation of several oxidation states in the aqueous phase, molybdenum chemistry is rather complicated. Depending on the acidity of the aqueous solution, the size and type of molybdenum ion change [31]. However, the cationic molybdenum may form at a low pH range that describes the high Mo extraction values in Figure 3a. Conversely, little amounts of Re are extracted at the same low pH range, which is correlated to the existence of Re in its ReO_4^- form that is not extractable by PC88A (Figure 3b). It can be inferred from Figure 3a,b that by keeping the concentration of PC88A constant and changing proton concentration, selectivity increases towards Mo extraction over Re.

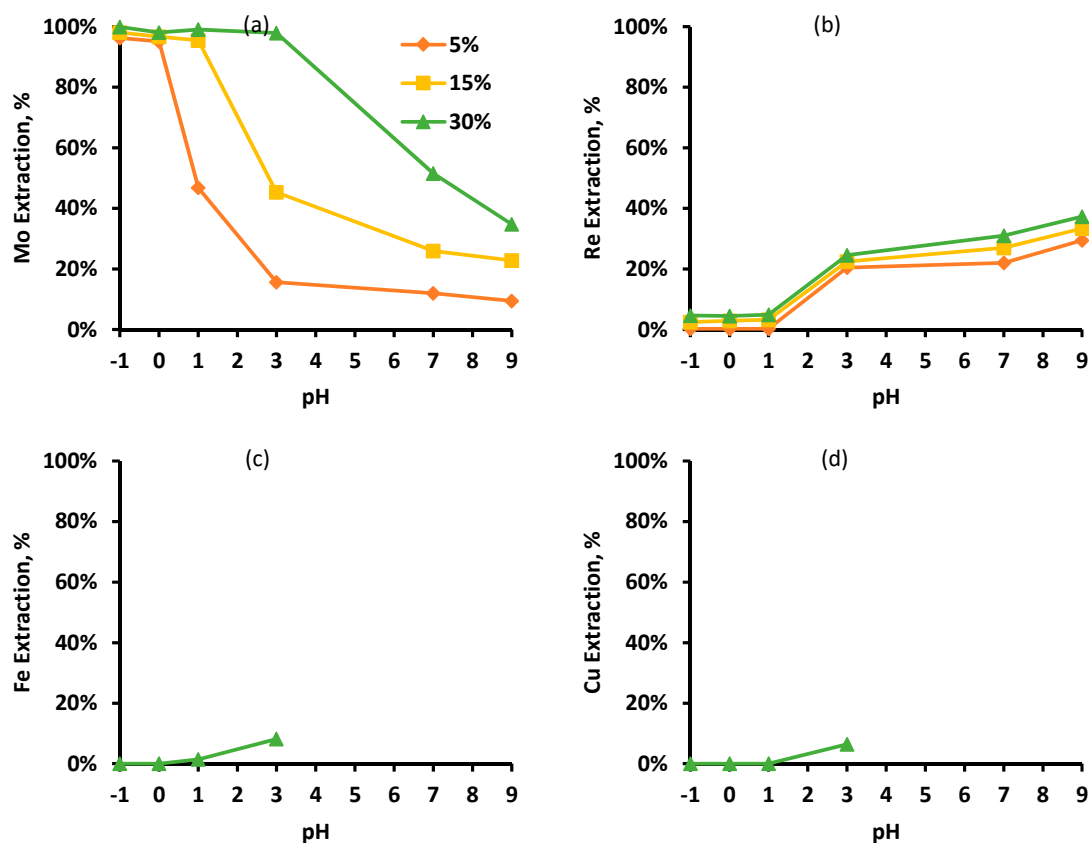


Figure 3. Metal extraction profiles as a function of pH and organic phase concentration: (a) Re, (b) Mo, (c) Fe, and (d) Cu.

Likewise, the effect of PC88A concentration on the extraction of Mo and Re was studied. However, for the case of Fe and Cu extraction, this effect was not studied (one-time test using 30% PC88A). It is clear that in the pH range of 1 to 3, increasing extractant concentrations does effectively change the Mo–Re extraction help in a better separation, notably near pH = 1.

3.2. Effect of Extractant

The organophosphoric acid reagents PC88A and D2EHPA are close analogs. Metal extraction at pH = 1, 3, and 7 was performed using an organic phase composed of 15% D2EHPA diluted in kerosene to be compared with PC88A. Experimental results show that PC88A is highly selective in the extraction of Mo over Re at pH = 1, while D2EHPA is more capable of providing a noticeable separation at neutral pH (Table 4).

Table 4. Comparison of PC88A and D2EHPA capability of separation between Re and Mo.

Extractant	pH	Org. Conc.	Mo Recovery (%)	Re Recovery (%)
PC88A	1	15	95.48	3.19
D2EHPA	1	15	81.51	15.35
PC88A	3	15	45.32	22.45
D2EHPA	3	15	57.23	4.3
PC88A	7	15	25.94	27
D2EHPA	7	15	90.08	14.1

Such observed behaviours could be attributed to the Re and Mo species properties and the properties of the extractants (PC88A and D2EHPA) over the entire range of studied pH. To disclose the effects of these parameters on the separation of Mo over Re, first, the properties of the two extractants were studied via DFT calculations. Figures 4 and 5 display the converged structures of the two extractants along with the distributions of their highest occupied molecular orbitals (HOMOs) and lowest unoccupied molecular orbitals (LUMOs).

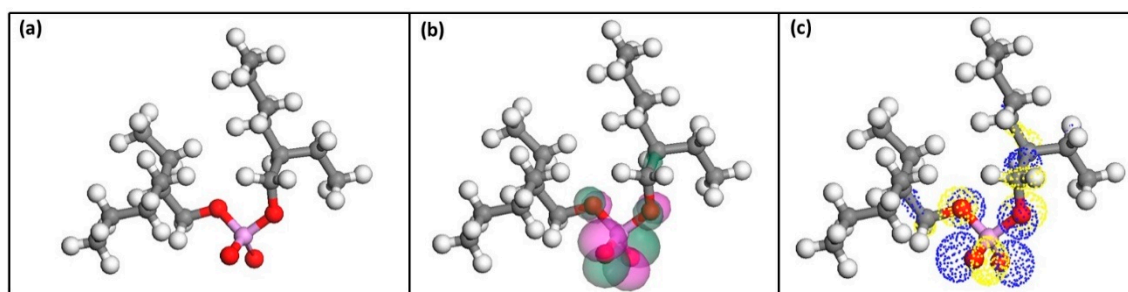


Figure 4. (a) Optimised structure of D2EHPA, (b) distribution of highest occupied molecular orbitals (HOMOs) of D2EHPA, and (c) distribution of lowest unoccupied molecular orbitals (LUMOs) of D2EHPA.

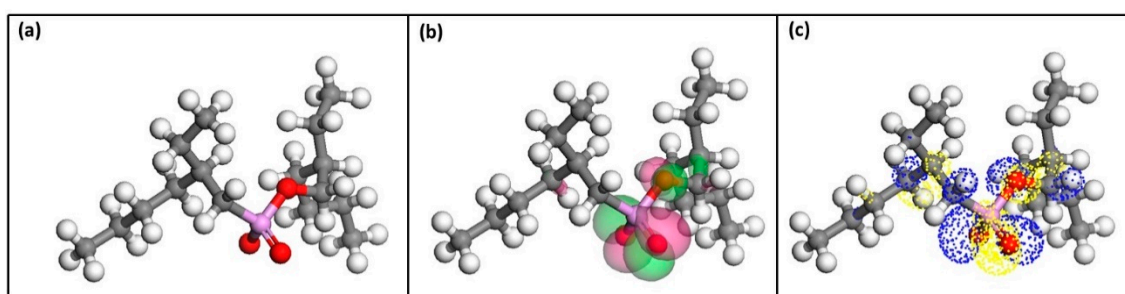


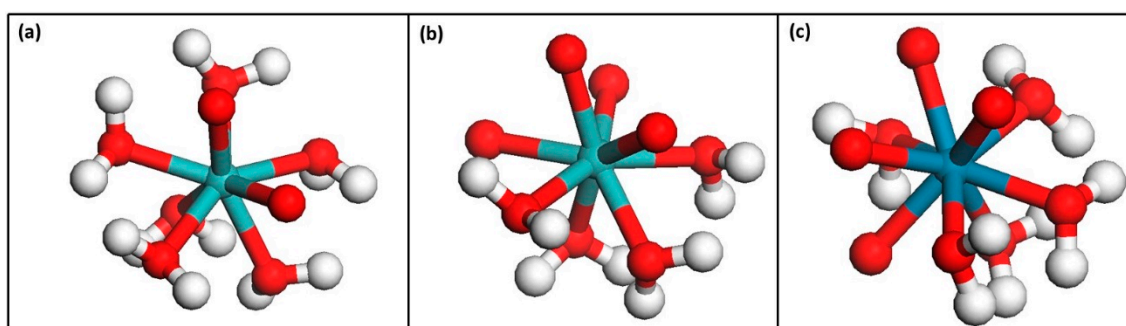
Figure 5. (a) Optimised structure of PC88A, (b) distribution of highest occupied molecular orbitals (HOMOs) of PC88A, and (c) distribution of lowest unoccupied molecular orbitals (LUMOs) of PC88A.

As seen, HOMOs and LUMOs are mostly located around their P = O and P – O groups, which are considered polar electron donor groups in the structure of these extractants. Furthermore, a Hirshfeld charge analysis was performed to assess the electronic charge of O atoms in P = O and P – O groups as presented in Table 5.

Table 5. Charge properties of PC88A and D2EHPA.

Extractants	Active Group	Charge (e)	Average Charge (e)
D2EHPA	P = O	−0.551	−0.552
	P − O	−0.553	
PC88A	P = O	−0.54	−0.545
	P − O	−0.53	

As illustrated in the Table 5, more electronic charges accumulate in both polar groups of D2EHPA, which are responsible for the complex formation through solvent extraction. This means that D2EHPA can be considered a stronger extractant, while PC88A has a potential for being a more selective reagent through solvent extraction. Such behaviour of these two extractants has already been reported in the literature [32]. Considering that the pK_a of D2EHPA and that of PC88A are around 3.01 and 4.21, respectively [33], this implies that these extractants will lie in their molecular forms for $pH \leq pK_a$ and will be dissociated into their ionic forms outside this pH range. In addition to extractant properties, Re and Mo species and properties are varied at studied pH as demonstrated in Figure 2. Variations in pH should play a critical role through complex formations in the present solvent extraction system. In this regard, as seen in Figure 2, while ReO_4^- can be considered a dominated Re species over the entire range of studied pH, MoO_2^{2+} at pH = 1, $Mo_7O_{24}^{6-}$ and $Mo_8O_{26}^{4-}$ at pH = 3, and MoO_4^{2-} at natural pH are regarded as dominated Mo species. Water-solvated forms of ReO_4^- , MoO_4^{2-} , and MoO_2^{2+} were studied by DFT calculations (Figure 6) to disclose more details about these Re and Mo species. It was found that ReO_4^- , MoO_4^{2-} , and MoO_2^{2+} are solvated with five, four, and seven water molecules, respectively. It was also realised that bond lengths of water- ReO_4^- are less than others (Table 6), indicating stronger interactions between water molecules and ReO_4^- as compared with those involved with the Mo species. Besides, Hirshfeld charge analysis was performed to compare charges of Re and Mo in these three species after solvation. It was realised that changes in the charge of Re are higher compared with those of Mo after solvation (water) of these three species as presented in Table 6, indicating higher interaction between water molecules and ReO_4^- as already established through bond length assessments.

**Figure 6.** Optimised structures of (a) MoO_2^{2+} , (b) MoO_4^{2-} , and (c) ReO_4^- .**Table 6.** Charge analysis and bond length of solvated Re and Mo species in the aqueous phase.

Species	Charge e (Re or Mo)		Changes (e)	Water Bond Length (Å)
	Nonsolvated	Solvated		
MoO_4^{2-}	0.83	0.61	0.22	2.3
MoO_2^{2+}	0.89	0.6	0.29	2.3
ReO_4^-	0.74	0.4	0.34	2.2

As seen in Table 4, PC88A performance in Mo extraction decreased once pH increased. At pH = 1, PC88A is in molecular form, but positively charged Mo species, MoO_2^{2+} , with relatively low

interaction with water molecule is the prevailing species. Therefore, making bond between PC88A and MoO_2^{2+} occurred. On the other hand, at pH = 3, relatively bulky species of Mo, including $\text{Mo}_7\text{O}_{24}^{6-}$ and $\text{Mo}_8\text{O}_{26}^{4-}$, are predicted to be the dominant forms in the solution, while the extractant is in its molecular form. It may be speculated that hindrance effects prevent bond formations between Mo species and PC88A, thus the declining recovery of Mo. Finally, at pH = 7, negatively charged MoO_4^{2-} forms along with PC88A dissociated into its ionic moieties. In this situation, it is suggested that electrostatic repulsions hinder the bond formation. Such effect can be more pronounced when it is noticed that PC88A is not a strong extractant based on DFT calculations. However, the case of Re is different as its recovery increased with increasing pH. Over the entire range of studied pH, Re is in the form of ReO_4^- , showcasing strong interactions with water molecules. PC88A dissociates in its ionic constituents with a potential for bond formation only at pH 7. Hence, it can be speculated that at pH 7, PC88A was more likely to create bonds with the Re species. Even in this situation, it is worthy to mention that PC88A is not a strong extractant based on DFT calculations; thus, although enhancement in Re recovery occurred through pH evolution, generally, its recovery is relatively lower than that of Mo in all ranges of pH. This could be due to the strength degree of PC88A in bond formation and the stability of ReO_4^- in interaction with water molecules. In the case of D2EHPA, hindrance effect at pH = 3 and repulsion at pH = 7 are less pronounced through Mo separation due to its stronger capability in complex formation (according to DFT calculations).

In order to confirm these explanations for the solvent extraction system, the interaction energy of the extractants with the Re and Mo species were obtained and are reported in Table 7. Interactions in both the organic and aqueous phases were taken into consideration since complexations could occur in both environments. In the case of aqueous phase calculations, the water-solvated forms of the species were considered. As seen in Table 7, the interaction energies of D2EHPA are higher than those of PC88A, which could be due to its stronger capability for complex formation. Besides, it can be seen that the interaction energies of both extractants follow this trend considering the Mo species: $\text{MoO}_2^{2+} > \text{MoO}_4^{2-}$. This trend is in line with the observation in Table 4. Besides, the interaction energies of D2EHPA and PC88A with the species are based on these trends, respectively: $\text{MoO}_2^{2+} > \text{MoO}_4^{2-} > \text{ReO}_4^-$ and $\text{MoO}_2^{2+} > \text{ReO}_4^- > \text{MoO}_4^{2-}$. These are also in line with observed recovery at different pH values.

Table 7. Interaction energy (kJ/mol) species with extractants in the organic and aqueous phases.

Species	PC88A		D2EHPA	
	Organic	Aqueous	Organic	Aqueous
MoO_4^{2-}	-178.1	-138.1	-321.3	-237.5
MoO_2^{2+}	-411.4	-321.1	-372.1	-221.8
ReO_4^-	-189.1	-155.3	-195.3	-157.1

4. Conclusions

PC88A was found to be a suitable solvent extraction candidate for selectively removing Mo over Re from molybdenite flue dust leach solutions. Acidifying the leach solution with H_2SO_4 at pH = 0–1 and employing an organic phase composed of 10–15% PC88A diluted in kerosene led to an ultimate separation between Mo and Re, transferring ca. 97% of Mo to the organic phase and leaving ca. 98% of Re in the leach solution. DFT simulations also indicated that the interaction energies of metals with D2EHPA were stronger than those with PC88A, thus explaining a different capability for complex formation. Besides, considering the Mo species, it was found that the interaction energies of both extractants followed the trend $\text{MoO}_2^{2+} > \text{MoO}_4^{2-}$ in line with the experimental observations. It was also confirmed via DFT simulations that the interaction energies of D2EHPA and PC88A with the metal oxyspecies follow the trends $\text{MoO}_2^{2+} > \text{MoO}_4^{2-} > \text{ReO}_4^-$ and $\text{MoO}_2^{2+} > \text{ReO}_4^- > \text{MoO}_4^{2-}$, respectively. These are also in line with observed recoveries at different pH values.

Author Contributions: Conceptualization, A.E.-Z.; data curation, A.E.-Z., D.A., P.A.N., F.L., and L.-C.P.; formal analysis, A.E.-Z. and D.A.; methodology, A.E.-Z.; project administration, F.L.; software, P.A.N.; writing—original draft, A.E.-Z.; writing—review and editing, D.A., P.A.N., F.L., and L.-C.P. All authors have read and agreed to the published version of the manuscript.

Funding: This research received no external funding.

Acknowledgments: The authors are grateful to the Babakan Ferromolybdenum Co. and Ali Amirarmand (Yazd Science and Technology Park) for providing the materials.

Conflicts of Interest: The authors declare no conflict of interest.

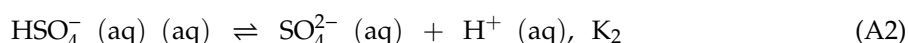
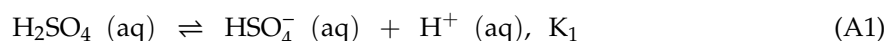
Appendix A Appearance of the Leaching Solution



Figure A1. The solution colour changes in the course of molybdenite flue dust leaching. It first became pale yellow (right), then turned into green, and finally dark blue (left).

Appendix B Details of the Thermodynamic Calculations

In order to construct the potential–pH diagram (Figure 2), the thermodynamic activities of ionic species in the solution should be calculated. To do it, the composition of the leaching solution should be estimated first. The leaching reactions of molybdenite flue dust are described by Equations (1)–(4). According to them, the primary aqueous species for Mo and Re are MoO_2^{2+} and ReO_4^- , respectively. Sulphuric acid is used to maintain the desired pH value. However, it is dibasic; it does not dissociate completely and may form sulphate and hydrosulphate ions and undissociated H_2SO_4 in the solution according to the following equations:



The dissociation constants are presented in Table A1.

Table A1. Dissociation constants of sulphuric acid at 25 °C.

Step i	K_i , mol/L	Reference
1	1000	[34]
2	0.012	[35]

Let $c_{\text{H}_2\text{SO}_4}^0$ be the initial concentration of sulphuric acid and $c_{\text{H}_2\text{SO}_4}$, $c_{\text{HSO}_4^-}$, and $c_{\text{SO}_4^{2-}}$ the equilibrium concentrations of different species. Then the following equations for the equilibrium constants may be written:

$$K_2 = \frac{c_{\text{SO}_4^{2-}} \cdot c_{\text{H}^+}}{c_{\text{HSO}_4^-}} \quad (\text{A3})$$

$$K_1 = \frac{c_{\text{HSO}_4^-} \cdot c_{\text{H}^+}}{c_{\text{H}_2\text{SO}_4}} \quad (\text{A4})$$

$$c_{\text{H}_2\text{SO}_4}^{\circ} = c_{\text{H}_2\text{SO}_4} + c_{\text{HSO}_4^-} + c_{\text{SO}_4^{2-}} \quad (\text{A5})$$

Rearranging Equations (A3) and (A4) and substituting them into Equation (A5) yields

$$c_{\text{HSO}_4^-} = \frac{c_{\text{SO}_4^{2-}} \cdot c_{\text{H}^+}}{K_2} \quad (\text{A6})$$

$$c_{\text{H}_2\text{SO}_4} = \frac{c_{\text{HSO}_4^-} \cdot c_{\text{H}^+}}{K_1} = \frac{\frac{c_{\text{SO}_4^{2-}} \cdot c_{\text{H}^+}}{K_2} \cdot c_{\text{H}^+}}{K_1} = \frac{c_{\text{SO}_4^{2-}} \cdot c_{\text{H}^+}^2}{K_1 \cdot K_2} \quad (\text{A7})$$

$$c_{\text{H}_2\text{SO}_4}^{\circ} = \frac{c_{\text{SO}_4^{2-}} \cdot c_{\text{H}^+}^2}{K_1 \cdot K_2} + \frac{c_{\text{SO}_4^{2-}} \cdot c_{\text{H}^+}}{K_2} + c_{\text{SO}_4^{2-}} \quad (\text{A8})$$

Rearranging Equation (A8) gives

$$c_{\text{H}_2\text{SO}_4}^{\circ} = c_{\text{SO}_4^{2-}} \cdot \left(\frac{c_{\text{H}^+}^2}{K_1 \cdot K_2} + \frac{c_{\text{H}^+}}{K_2} + 1 \right) \quad (\text{A9})$$

$$c_{\text{H}_2\text{SO}_4}^{\circ} = c_{\text{SO}_4^{2-}} \cdot \left(\frac{c_{\text{H}^+}^2}{K_1 \cdot K_2} + \frac{K_1 \cdot c_{\text{H}^+}}{K_1 \cdot K_2} + \frac{K_1 \cdot K_2}{K_1 \cdot K_2} \right) \quad (\text{A10})$$

$$c_{\text{H}_2\text{SO}_4}^{\circ} = c_{\text{SO}_4^{2-}} \cdot \frac{c_{\text{H}^+}^2 + K_1 \cdot c_{\text{H}^+} + K_1 \cdot K_2}{K_1 \cdot K_2} \quad (\text{A11})$$

$$K_1 \cdot K_2 \cdot c_{\text{H}_2\text{SO}_4}^{\circ} = c_{\text{SO}_4^{2-}} \cdot (c_{\text{H}^+}^2 + K_1 \cdot c_{\text{H}^+} + K_1 \cdot K_2) \quad (\text{A12})$$

$$c_{\text{SO}_4^{2-}} = \frac{K_1 \cdot K_2 \cdot c_{\text{H}_2\text{SO}_4}^{\circ}}{c_{\text{H}^+}^2 + K_1 \cdot c_{\text{H}^+} + K_1 \cdot K_2} \quad (\text{A13})$$

The equilibrium concentrations of hydrosulphate ions and undissociated sulphuric acid might be obtained by substituting Equation (A13) into Equations (A6) and (A7):

$$c_{\text{HSO}_4^-} = \frac{c_{\text{SO}_4^{2-}} \cdot c_{\text{H}^+}}{K_2} = \frac{\frac{K_1 \cdot K_2 \cdot c_{\text{H}_2\text{SO}_4}^{\circ}}{c_{\text{H}^+}^2 + K_1 \cdot c_{\text{H}^+} + K_1 \cdot K_2} \cdot c_{\text{H}^+}}{K_2} = \frac{K_1 \cdot c_{\text{H}^+} \cdot c_{\text{H}_2\text{SO}_4}^{\circ}}{c_{\text{H}^+}^2 + K_1 \cdot c_{\text{H}^+} + K_1 \cdot K_2} \quad (\text{A14})$$

$$c_{\text{H}_2\text{SO}_4} = \frac{c_{\text{SO}_4^{2-}} \cdot c_{\text{H}^+}^2}{K_1 \cdot K_2} = \frac{\frac{K_1 \cdot K_2 \cdot c_{\text{H}_2\text{SO}_4}^{\circ}}{c_{\text{H}^+}^2 + K_1 \cdot c_{\text{H}^+} + K_1 \cdot K_2} \cdot c_{\text{H}^+}^2}{K_1 \cdot K_2} = \frac{c_{\text{H}^+}^2 \cdot c_{\text{H}_2\text{SO}_4}^{\circ}}{c_{\text{H}^+}^2 + K_1 \cdot c_{\text{H}^+} + K_1 \cdot K_2} \quad (\text{A15})$$

Let us introduce the mole fractions of the three species in the solution:

$$x_{\text{SO}_4^{2-}} = \frac{n_{\text{SO}_4^{2-}}}{n_{\text{H}_2\text{SO}_4} + n_{\text{HSO}_4^-} + n_{\text{SO}_4^{2-}}} \quad V = \text{const} \quad \frac{c_{\text{SO}_4^{2-}}}{c_{\text{H}_2\text{SO}_4} + c_{\text{HSO}_4^-} + c_{\text{SO}_4^{2-}}} = \frac{c_{\text{SO}_4^{2-}}}{c_{\text{H}_2\text{SO}_4}^{\circ}} \quad (\text{A16})$$

$$x_{\text{HSO}_4^-} = \frac{n_{\text{HSO}_4^-}}{n_{\text{H}_2\text{SO}_4} + n_{\text{HSO}_4^-} + n_{\text{SO}_4^{2-}}} \quad V = \text{const} \quad \frac{c_{\text{HSO}_4^-}}{c_{\text{H}_2\text{SO}_4} + c_{\text{HSO}_4^-} + c_{\text{SO}_4^{2-}}} = \frac{c_{\text{HSO}_4^-}}{c_{\text{H}_2\text{SO}_4}^{\circ}} \quad (\text{A17})$$

$$x_{\text{H}_2\text{SO}_4} = \frac{n_{\text{H}_2\text{SO}_4}}{n_{\text{H}_2\text{SO}_4} + n_{\text{HSO}_4^-} + n_{\text{SO}_4^{2-}}} \quad V = \text{const} \quad \frac{c_{\text{H}_2\text{SO}_4}}{c_{\text{H}_2\text{SO}_4} + c_{\text{HSO}_4^-} + c_{\text{SO}_4^{2-}}} = \frac{c_{\text{H}_2\text{SO}_4}}{c_{\text{H}_2\text{SO}_4}^{\circ}} \quad (\text{A18})$$

Consequently,

$$x_{\text{SO}_4^{2-}} = \frac{c_{\text{SO}_4^{2-}}}{c_{\text{H}_2\text{SO}_4}^0} = \frac{K_1 \cdot K_2 \cdot c_{\text{H}_2\text{SO}_4}^0}{c_{\text{H}^+}^2 + K_1 \cdot c_{\text{H}^+} + K_1 \cdot K_2} = \frac{K_1 \cdot K_2}{c_{\text{H}^+}^2 + K_1 \cdot c_{\text{H}^+} + K_1 \cdot K_2} \quad (\text{A19})$$

$$x_{\text{HSO}_4^-} = \frac{c_{\text{HSO}_4^-}}{c_{\text{H}_2\text{SO}_4}^0} = \frac{K_1 \cdot c_{\text{H}^+} \cdot c_{\text{H}_2\text{SO}_4}^0}{c_{\text{H}^+}^2 + K_1 \cdot c_{\text{H}^+} + K_1 \cdot K_2} = \frac{K_1 \cdot c_{\text{H}^+}}{c_{\text{H}^+}^2 + K_1 \cdot c_{\text{H}^+} + K_1 \cdot K_2} \quad (\text{A20})$$

$$x_{\text{H}_2\text{SO}_4} = \frac{c_{\text{H}_2\text{SO}_4}}{c_{\text{H}_2\text{SO}_4}^0} = \frac{c_{\text{H}^+}^2 \cdot c_{\text{H}_2\text{SO}_4}^0}{c_{\text{H}^+}^2 + K_1 \cdot c_{\text{H}^+} + K_1 \cdot K_2} = \frac{c_{\text{H}^+}^2}{c_{\text{H}^+}^2 + K_1 \cdot c_{\text{H}^+} + K_1 \cdot K_2} \quad (\text{A21})$$

It is worth noting that

$$x_{\text{H}_2\text{SO}_4} + x_{\text{HSO}_4^-} + x_{\text{SO}_4^{2-}} = 1 \quad (\text{A22})$$

If the pH value is predetermined and the values of the equilibrium constants K_1 and K_2 (see Equations (A3) and (A4)), are known, the mole fractions of the three species in the solution might be unambiguously calculated. The dependency of the mole fractions of the species on pH value is called the speciation diagram. The speciation diagram for the sulphuric acid is presented in Figure A2.

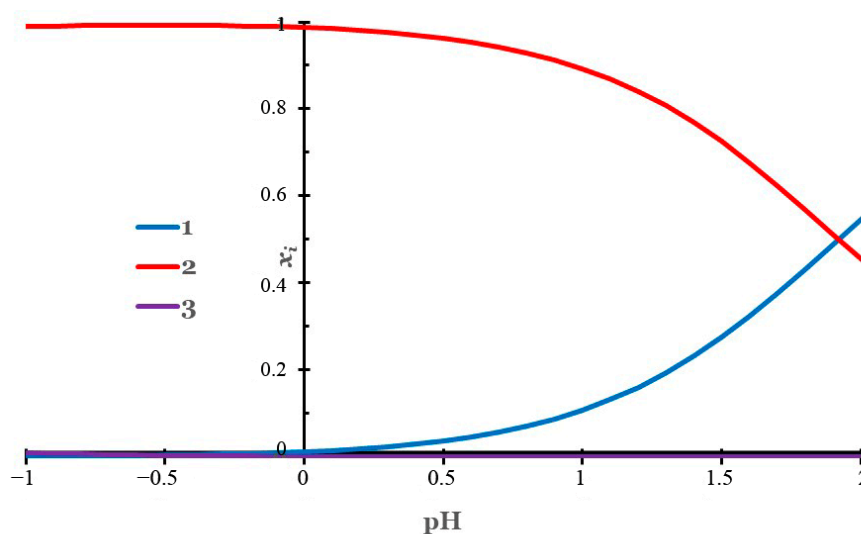


Figure A2. The speciation diagram for the sulphuric acid in the pH range from -1 to 2 . (1)— SO_4^{2-} (aq), (2)— HSO_4^- (aq), (3)— H_2SO_4 (aq).

Because pH is not an independent variable and is determined by the addition of sulphuric acid, one needs to estimate the relationship between the total content of sulphuric acid in the solution and the pH value. To do it, the material balance equations should be considered.

In the first dissociation step (Equation (A1)), let the initial concentration of sulphuric acid be $c_{\text{H}_2\text{SO}_4}^0$. Let x moles of free acid per litre of solution dissociate to hydrosulphate ions. Consequently, the equilibrium concentration of the hydrosulphate ions is equal to x . From the reaction stoichiometry, it follows that the equilibrium concentration of hydrogen ions according to that dissociation step is also equal to x .

In the second dissociation step (Equation (A2)), let y moles of hydrosulphate ions per litre of solution dissociate further to sulphate ions. Consequently, the equilibrium concentration of the sulphate ions is equal to y . From the reaction stoichiometry, it follows that the equilibrium concentration of hydrogen ions according to that dissociation step is also equal to y .

Considering both dissociation steps, one might notice that the equilibrium concentration of hydrogen ions according to both dissociation steps equals $x + y$, the equilibrium concentration of hydrosulphate ions equals $x - y$, and the equilibrium concentration of free acid equals $c_{\text{H}_2\text{SO}_4}^0 - x$ (see Table A2).

Table A2. Material balance of sulphuric acid dissociation.

	H_2SO_4 (aq)	\rightleftharpoons	HSO_4^- (aq)	+	H^+ (aq)
Initial state	$c_{\text{H}_2\text{SO}_4}^0$		0		0
Equilibrium state	$c_{\text{H}_2\text{SO}_4}^0 - x$		x		x
	HSO_4^- (aq)	\rightleftharpoons	SO_4^{2-} (aq)	+	H^+ (aq)
Initial state	x		0		x
Equilibrium state	$x - y$		y		$x + y$

If the pH value is known, the ratio of equilibrium concentrations of sulphate and hydrosulphate ions is constant. The following system of equations may be written:

$$c_{\text{H}^+} = 10^{-\text{pH}} = x + y \quad (\text{A23})$$

$$\frac{c_{\text{HSO}_4^-}}{c_{\text{SO}_4^{2-}}} = \frac{x - y}{y} \quad (\text{A24})$$

Rearranging Equation (A24) yields

$$\frac{x - y}{y} = \frac{x}{y} - 1 = \frac{c_{\text{HSO}_4^-}}{c_{\text{SO}_4^{2-}}} \quad (\text{A25})$$

$$\frac{x}{y} = \frac{c_{\text{HSO}_4^-}}{c_{\text{SO}_4^{2-}}} + 1 \quad (\text{A26})$$

$$x = y \cdot \left(\frac{c_{\text{HSO}_4^-}}{c_{\text{SO}_4^{2-}}} + 1 \right) \quad (\text{A27})$$

$$c_{\text{H}^+} = x + y = y \cdot \left(\frac{c_{\text{HSO}_4^-}}{c_{\text{SO}_4^{2-}}} + 1 \right) + y = y \cdot \left(\frac{c_{\text{HSO}_4^-}}{c_{\text{SO}_4^{2-}}} + 2 \right) \quad (\text{A28})$$

$$y = \frac{c_{\text{H}^+}}{\frac{c_{\text{HSO}_4^-}}{c_{\text{SO}_4^{2-}}} + 2} \quad (\text{A29})$$

Obviously, the ratio of equilibrium concentrations of sulphate and hydrosulphate ions is equal to the ratio of their mole fractions:

$$\frac{c_{\text{HSO}_4^-}}{c_{\text{SO}_4^{2-}}} = \frac{x_{\text{HSO}_4^-}}{x_{\text{SO}_4^{2-}}} = \frac{K_1 \cdot c_{\text{H}^+}}{c_{\text{H}^+}^2 + K_1 \cdot c_{\text{H}^+} + K_1 \cdot K_2} : \frac{K_1 \cdot K_2}{c_{\text{H}^+}^2 + K_1 \cdot c_{\text{H}^+} + K_1 \cdot K_2} = \frac{K_1 \cdot c_{\text{H}^+}}{K_1 \cdot K_2} = \frac{c_{\text{H}^+}}{K_2} \quad (\text{A30})$$

Substituting Equation (A30) into Equation (A29) gives

$$y = c_{\text{SO}_4^{2-}} = \frac{c_{\text{H}^+}}{\frac{c_{\text{HSO}_4^-}}{c_{\text{SO}_4^{2-}}} + 2} = \frac{c_{\text{H}^+}}{\frac{c_{\text{H}^+}}{K_2} + 2} = \frac{K_2 \cdot c_{\text{H}^+}}{c_{\text{H}^+} + 2 \cdot K_2} \quad (\text{A31})$$

Substituting Equation (A31) into Equations (A6) and (A7) yields

$$c_{\text{HSO}_4^-} = \frac{c_{\text{SO}_4^{2-}} \cdot c_{\text{H}^+}}{K_2} = \frac{\frac{K_2 \cdot c_{\text{H}^+}}{c_{\text{H}^+} + 2 \cdot K_2} \cdot c_{\text{H}^+}}{K_2} = \frac{c_{\text{H}^+}^2}{c_{\text{H}^+} + 2 \cdot K_2} \quad (\text{A32})$$

$$c_{\text{H}_2\text{SO}_4} = \frac{c_{\text{SO}_4^{2-}} \cdot c_{\text{H}^+}^2}{K_1 \cdot K_2} = \frac{\frac{K_2 \cdot c_{\text{H}^+}}{c_{\text{H}^+} + 2 \cdot K_2} \cdot c_{\text{H}^+}^2}{K_1 \cdot K_2} = \frac{c_{\text{H}^+}^3}{c_{\text{H}^+} \cdot K_1 + 2 \cdot K_1 \cdot K_2} \quad (\text{A33})$$

Therefore, by using Equations (A5) and (A31)–(A33), the equilibrium concentrations of different species and the total content of sulphuric acid at the given pH value might be calculated straightforwardly. The calculated concentrations for pH values equal to 2, 1, 0, and −1 are presented in Table A3.

Table A3. Equilibrium concentrations of various aqueous sulphuric acid species and total concentration of sulphuric acid at different pH values.

PH	$c_{\text{H}_2\text{SO}_4}$, mol/L	$c_{\text{HSO}_4^-}$, mol/L	$c_{\text{SO}_4^{2-}}$, mol/L	$c_{\text{H}_2\text{SO}_4}^0$, mol/L
2	2.94×10^{-8}	0.00294	0.00353	0.00647
1	8.06×10^{-6}	0.0806	0.00968	0.0903
0	0.000977	0.977	0.0117	0.989
−1	0.0998	9.976	0.0119	10.088

The leaching reactions of molybdenite flue dust are given by reactions (1) through (4). According to them, the aqueous species to molybdenum and rhenium in the leaching liquor are MoO_2^{2+} and ReO_4^- , respectively. According to Table 3, the total content of molybdenum in a solution equals:

$$c_{[\text{Mo}]} = 9 \frac{\text{g}}{\text{L}} : 95.94 \frac{\text{g}}{\text{mol}} = 0.094 \frac{\text{mol}}{\text{L}} \quad (\text{A34})$$

The total content of rhenium equals:

$$c_{[\text{Re}]} = 0.5 \frac{\text{g}}{\text{L}} : 186.207 \frac{\text{g}}{\text{mol}} = 0.0027 \frac{\text{mol}}{\text{L}} \quad (\text{A35})$$

The parameters of the extended Debye–Hückel equation are:

$$T = 298.15 \text{ K} \quad (\text{A36})$$

$$\varepsilon = 87.74 - 0.4008 \cdot (T - 273.15) + 9.398 \cdot 10^{-4} \cdot (T - 273.15)^2 + 1.41 \cdot 10^{-6} \cdot (T - 273.15)^3 = 78.3294 \quad (\text{A37})$$

$$A = \frac{1.825 \cdot 10^6}{(\varepsilon \cdot T)^{\frac{3}{2}}} = \frac{1.825 \cdot 10^6}{(78.3294 \cdot 298.15)^{\frac{3}{2}}} = 0.5114 \frac{\text{L}^{\frac{1}{2}}}{\text{mol}^{\frac{1}{2}}} \quad (\text{A38})$$

$$B = \frac{5.029 \cdot 10^{11}}{(\varepsilon \cdot T)^{\frac{1}{2}}} = \frac{5.029 \cdot 10^{11}}{(78.3294 \cdot 298.15)^{\frac{1}{2}}} = 3.291 \cdot 10^9 \frac{\text{L}^{\frac{1}{2}}}{\text{m} \cdot \text{mol}^{\frac{1}{2}}} \quad (\text{A39})$$

The electrostatic radii of the individual ions are presented in Table A4.

Table A4. Electrostatic radii of individual ions.

Ion	a_i , Å
ReO_4^-	4.5
MoO_2^{2+}	4.5

The ionic strength of the solution is calculated as follows:

$$I = \frac{C_{\text{ReO}_4^-} \cdot z_{\text{ReO}_4^-}^2 + C_{\text{MoO}_2^{2+}} \cdot z_{\text{MoO}_2^{2+}}^2 + C_{\text{SO}_4^{2-}} \cdot z_{\text{SO}_4^{2-}}^2 + C_{\text{HSO}_4^-} \cdot z_{\text{HSO}_4^-}^2 + C_{\text{H}^+} \cdot z_{\text{H}^+}^2}{2} \quad (\text{A40})$$

The activity coefficients of molybdenum and rhenium ions in a solution are calculated according to the extended Debye–Hückel equation. The thermodynamic activities are calculated straightforwardly:

$$\lg \gamma_{\text{ReO}_4^-} = -A \cdot z_{\text{ReO}_4^-}^2 \cdot \frac{\sqrt{I}}{1 + B \cdot a_{\text{ReO}_4^-} \cdot \sqrt{I}} \quad (\text{A41})$$

$$a_{\text{ReO}_4^-} = c_{[\text{Re}]} \cdot 10^{\gamma_{\text{ReO}_4^-}} \quad (\text{A42})$$

$$\lg \gamma_{\text{MoO}_2^{2+}} = -A \cdot z_{\text{MoO}_2^{2+}}^2 \cdot \frac{\sqrt{I}}{1 + B \cdot a_{\text{MoO}_2^{2+}} \cdot \sqrt{I}} \quad (\text{A43})$$

$$a_{\text{MoO}_2^{2+}} = c_{[\text{Mo}]} \cdot 10^{\gamma_{\text{MoO}_2^{2+}}} \quad (\text{A44})$$

The calculated values are presented in Table A5.

Table A5. Activity coefficients and thermodynamic activities of molybdenum and rhenium species in leaching stock solution at different pH values.

pH	I, mol/L	lg $\gamma_{\text{ReO}_4^-}$	$a_{\text{ReO}_4^-}$, mol/L	lg $\gamma_{\text{MoO}_2^{2+}}$	$a_{\text{MoO}_2^{2+}}$, mol/L
2	0.20288	−0.138	0.00196	−0.553	0.0263
1	0.299	−0.155	0.00189	−0.618	0.0226
0	1.096	−0.214	0.00165	−0.855	0.0131
−1	10.201	−0.285	0.00140	−1.140	0.0068

As can be seen, the average activities of the molybdenum species are ~0.01 mol/L, and those of the rhenium species are ~0.001 mol/L. The activities of the sulphur species have no influence on the position of the lines on the diagram.

The potential–pH diagram for the Mo–Re–SO₄^{2−} system (Figure 2) is plotted at 25 °C, air pressure of 1 bar and the activities of the molybdenum species 0.01 mol/L, the activities of the rhenium species 0.001 mol/L, and the activities of the sulphur species 0.1 mol/L.

References

- Habashi, F. *Handbook of Extractive Metallurgy*; Wiley-VCH: Weinheim/Heidelberg, Germany, 1997.
- Virolainen, S.; Laatikainen, M.; Sainio, T. Ion exchange recovery of rhenium from industrially relevant sulfate solutions: Single column separations and modeling. *Hydrometallurgy* **2015**, *158*, 74–82. [[CrossRef](#)]
- Srivastava, R.R.; Lee, J.-C.; Kim, M.-S. Complexation chemistry in liquid–liquid extraction of rhenium. *J. Chem. Technol. Biotechnol.* **2015**, *90*, 1752–1764. [[CrossRef](#)]
- Cheema, H.A.; Ilyas, S.; Masud, S.; Muhsan, M.A.; Mahmood, I.; Lee, J.-C. Selective recovery of rhenium from molybdenite flue-dust leach liquor using solvent extraction with TBP. *Sep. Purif. Technol.* **2018**, *191*, 116–121. [[CrossRef](#)]
- Nikolaychuk, P.A.; Tyurin, A.G. Utočnënnââ diagramma Purbe dlâ molibdena. *Butlerovskie Soobšeniâ* **2011**, *24*, 101–105.
- Khoshnevisan, A.; Yoozbashizadeh, H.; Mohammadi, M.; Abazarpour, A.; Maarefvand, M. Separation of rhenium and molybdenum from molybdenite leach liquor by the solvent extraction method. *Miner. Metall. Process.* **2013**, *30*, 53–58. [[CrossRef](#)]

7. Alamdari, E.K.; Darvishi, D.; Haghshenas, D.F.; Yousefi, N.; Sadrnezhad, S.K. Separation of Re and Mo from roasting-dust leach-liquor using solvent extraction technique by TBP. *Sep. Purif. Technol.* **2012**, *86*, 143–148. [[CrossRef](#)]
8. Cao, Z.F.; Zhong, H.; Jiang, T.; Liu, G.Y.; Wang, S. Selective electric-oxidation leaching and separation of Dexing molybdenite concentrates. *Zhongguo Youse Jinshu Xuebao/Chin. J. Nonferrous Met.* **2013**, *23*, 2290–2295.
9. Zhan-fang, C.; Hong, Z.; Zhao-hui, Q. Solvent extraction of rhenium from molybdenum in alkaline solution. *Hydrometallurgy* **2009**, *97*, 153–157. [[CrossRef](#)]
10. Kang, J.; Kim, Y.U.; Joo, S.H.; Yoon, H.S.; Kumar, J.R.; Park, K.H.; Shin, S.M. Behavior of Extraction, Stripping, and Separation Possibilities of Rhenium and Molybdenum from Molybdenite Roasting Dust Leaching Solution Using Amine Based Extractant Tri-Otyl-Amine (TOA). *Mater. Trans.* **2013**, *54*, 1209–1212. [[CrossRef](#)]
11. Srivastava, R.R.; Kim, M.-S.; Lee, J.-C.; Ilyas, S. Liquid–liquid extraction of rhenium (VII) from an acidic chloride solution using Cyanex 923. *Hydrometallurgy* **2015**, *157*, 33–38. [[CrossRef](#)]
12. Pathak, S.K.; Singh, S.; Mahtele, A.; Tripathi, S.C. Studies on extraction behaviour of molybdenum (VI) from acidic radioactive waste using 2 (ethylhexyl) phosphonic acids, mono 2 (ethylhexyl) ester (PC-88A)/n-dodecane. *J. Radioanal. Nucl. Chem.* **2010**, *284*, 597–603. [[CrossRef](#)]
13. Wang, Y.; Jiang, K.; Zou, X.; Zhang, L.; Liu, S. Recovery of metals from molybdenite concentrate by hydrometallurgical technologies. In *TT Chen Honorary Symposium on Hydrometallurgy, Electrometallurgy and Materials Characterization*; John Wiley & Sons, Inc.: Hoboken, NJ, USA, 2012; pp. 315–322.
14. Nguyen, T.H.; Lee, M.S. Separation of molybdenum (VI) and tungsten (VI) from sulfate solutions by solvent extraction with LIX 63 and PC 88A. *Hydrometallurgy* **2015**, *155*, 51–55. [[CrossRef](#)]
15. Moris, M.A.A.; Díez, F.V.; Coca, J. Solvent extraction of molybdenum and tungsten by Alamine 336 and DEHPA in a rotating disc contactor. *Sep. Purif. Technol.* **1999**, *17*, 173–179. [[CrossRef](#)]
16. Truong, H.T.; Lee, M.S. Separation of rhenium (VII), molybdenum (VI), and vanadium (V) from hydrochloric acid solution by solvent extraction with TBP. *Geosyst. Eng.* **2017**, *20*, 224–230. [[CrossRef](#)]
17. Kim, H.S.; Park, J.S.; Seo, S.Y.; Tran, T.; Kim, M.J. Recovery of rhenium from a molybdenite roaster fume as high purity ammonium perhenate. *Hydrometallurgy* **2015**, *156*, 158–164. [[CrossRef](#)]
18. Xiao, C.; Zeng, L.; Xiao, L.; Zhang, G. Solvent Extraction of Molybdenum (VI) from Hydrochloric Acid Leach Solutions Using P507. Part I: Extraction and Mechanism. *Solvent Extr. Ion Exch.* **2017**, *156*, 130–144. [[CrossRef](#)]
19. Entezari, A.; Karamoozian, M.; Eskandari Nasab, M. Investigation on selective rhenium leaching from molybdenite roasting flue dusts. *J. Min. Environ.* **2013**, *4*, 77–82.
20. Entezari-Zarandi, A.; Larachi, F. Selective dissolution of rare-earth element carbonates in deep eutectic solvents. *J. Rare Earths* **2019**, *37*, 528–533. [[CrossRef](#)]
21. Keshavarz Alamdari, E. Selective Leaching-Recovery of Re and Mo from Out-Gas Dust of Molybdenite Roasting Furnace. *Trans. Indian Inst. Met.* **2017**, *70*, 1995–1999. [[CrossRef](#)]
22. Debye, P.; Hückel, E. Zur Theorie der Elektrolyte. I. Gefrierpunktserniedrigung und verwandte Erscheinungen. *Phys. Z* **1923**, *24*, 185–206.
23. Kielland, J. Individual activity coefficients of ions in aqueous solutions. *J. Am. Chem. Soc.* **1937**, *59*, 1675–1678. [[CrossRef](#)]
24. Coolidge, W. Dielektrische Untersuchungen und elektrische Drahtwellen. *Ann. Phys.* **1899**, *305*, 125–166. [[CrossRef](#)]
25. Nikolaychuk, P. Das revidierte pourbaix-diagramm für schwefel. In *Materialien Zum Wissenschaftlichen Seminar der Stipendiaten der Programme „Mikhail Lomonosov“ und „Immanuel Kant“*; Deutscher Akademischer Austausch Dienst und Ministerium für Bildung und Wissenschaft der RF: Moscow, Russia, 2015; pp. 72–76.
26. Wagman, D.D.; Evans, W.H.; Parker, V.B.; Schumm, R.H.; Halow, I. The NBS tables of chemical thermodynamic properties. Selected values for inorganic and C₁ and C₂ organic substances in SI units, National Standard Reference Data System. *J. Phys. Chem. Ref. Data* **1982**, *11*, 37–38.
27. Azizi, D.; Larachi, F. Behavior of bifunctional phosphonium-based ionic liquids in solvent extraction of rare earth elements-quantum chemical study. *J. Mol. Liq.* **2018**, *263*, 96–108. [[CrossRef](#)]
28. Palant, A.; Iatsenko, N.; Petrova, V. Solvent extraction of molybdenum (VI) by diisododecylamine from sulphuric acid solution. *Hydrometallurgy* **1998**, *48*, 83–90. [[CrossRef](#)]

29. Loewenschuss, A.; Shamir, J.; Ardon, M. Vibrational spectra of binuclear molybdenum sulfate complexes of high bond order. *Inorg. Chem.* **1976**, *15*, 238–241. [[CrossRef](#)]
30. Alamdari, E.K.; Sadrnezhad, S.K. Thermodynamics of extraction of from aqueous sulfuric acid media with TBP dissolved in kerosene. *Hydrometallurgy* **2000**, *55*, 327–341. [[CrossRef](#)]
31. Kholmogorov, A.G.; Kononova, O.N.; Panchenko, O.N. A Review of the Use of Ion Exchange for Molybdenum Recovery in Russia. *Can. Metall. Q.* **2004**, *43*, 297–304. [[CrossRef](#)]
32. Shi, Q.; Zhang, Y.; Huang, J.; Liu, T.; Liu, H.; Wang, L. Synergistic solvent extraction of vanadium from leaching solution of stone coal using D2EHPA and PC88A. *Sep. Purif. Technol.* **2017**, *181*, 1–7. [[CrossRef](#)]
33. Cheng, C.Y.; Barnard, K.R.; Zhang, W.; Robinson, D.J. Synergistic solvent extraction of nickel and cobalt: A review of recent developments. *Solvent Extr. Ion Exch.* **2011**, *29*, 719–754. [[CrossRef](#)]
34. Sue, K.; Uchids, M.; Adshiri, T.; Arai, K. Determination of sulfuric acid first dissociation constants to 400 °C and 32 MPa by potentiometric pH measurements. *J. Supercrit. Fluids* **2004**, *31*, 295–299. [[CrossRef](#)]
35. Wu, Y.C.; Feng, D. The second dissociation constant of sulfuric acid at various temperatures by the conductometric method. *J. Solut. Chem.* **1995**, *24*, 133–144. [[CrossRef](#)]

Publisher's Note: MDPI stays neutral with regard to jurisdictional claims in published maps and institutional affiliations.



© 2020 by the authors. Licensee MDPI, Basel, Switzerland. This article is an open access article distributed under the terms and conditions of the Creative Commons Attribution (CC BY) license (<http://creativecommons.org/licenses/by/4.0/>).